

Control of a Dual Stage Actuator System for Noncircular Cam Turning Process

Byung-Sub Kim
Department of Mechanical and
Industrial Engineering
University of Illinois at Urbana-Champaign
Urbana, IL 61801
bkim2@uiuc.edu

Jianwu Li
Lighting Technology
General Electric Company
Ravenna, OH 44266
Jianwu.Li@lighting.ge.com

Tsu-Chin Tsao
Mechanical and Aerospace
Engineering Department
University of California
Los Angeles, CA 90095
ttsao@seas.ucla.edu

Abstract

This paper presents a robust repetitive controller design for a dual stage actuator system for the noncircular cam turning process. The secondary actuator in this dual stage system is a piezoelectric actuator which is installed inside of the hollow piston of an electrohydraulic actuator. The controller is designed through a sequence of two SISO designs under the assumption that there is little interaction between two actuator systems. The error from the first stage electrohydraulic actuator is fed to the second stage piezoelectric actuator as reference. Therefore, the overall sensitivity function is effectively squared through two actuators and the total error is the same as the error coming from the piezoelectric actuator. Experimental results show the tracking performance improvement in noncircular cam turning application.

1 Introduction

Recently there has been increased interest in dual stage actuator systems to increase the bandwidth especially for magnetic hard disk drives. The prototype dual stage actuators in hard disk drive systems have another microactuator fabricated using MEMS fabrication techniques on the traditional voice coil motor actuator [1, 3]. The servo bandwidth of the second stage microactuator is much higher than that of the first stage voice coil motor. Research efforts have been focused on how to split the frequency components of reference signal to obtain cooperation between two actuators. The current dual stage actuator system used in this paper for the noncircular cam turning process consists of an electrohydraulic actuator and a piezoelectric actuator. The second stage piezoelectric actuator is installed inside of the hollow piston of the first stage electrohydraulic actuator. Figure 1 shows the cross sectional view of the dual stage actuator system. The spring plate flexure makes sure the piezoelectric actuator is in compression at all times and the piezoelectric actuator has a relative motion with respect to the electrohydraulic actuator. The traveling length of the electrohydraulic actuator is 25.4mm and the piezoelectric actu-

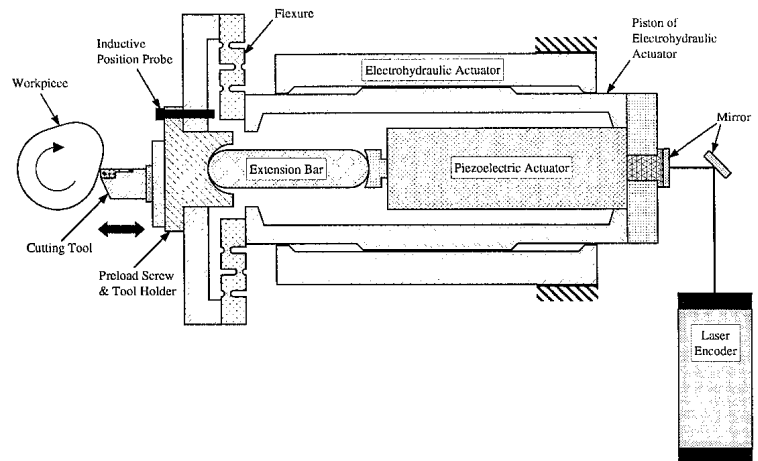


Figure 1: Cross Sectional View of Dual Stage Actuator System

ator has a $40\mu\text{m}$ stroke.

Unlike the aforementioned hard disk drive dual stage actuator system, the piezoelectric actuator used in this paper doesn't show a significantly large bandwidth compared with that of the electrohydraulic actuator because of the power amplifier saturation. Furthermore, most of the cam profiles have their dominant frequency components mainly in the low frequency range. Due to these reasons, dividing the control signal for two different actuators according to the error (or reference) frequency components is not a main controller design issue in this setup. The combination of an electrohydraulic actuator and a piezoelectric actuator is used in serial fashion to reduce the total error, i.e. the error from the primary electrohydraulic actuator is fed to the secondary piezoelectric actuator as reference. Thus, the overall sensitivity is squared in effect through two actuator systems. This paper is organized as follows. Section 2 discusses the modeling of the dual stage actuator system depicted in Figure 1. Section 3 presents the digital repetitive controller design for the dual stage servo system. Section 4 shows simulation and experimental results in the noncircular cam turning process. Finally, concluding remarks are given in Section 5.

2 Modeling of the Dual Stage Actuator System

A schematic dual stage actuator model is shown in Figure 2. The piezoelectric actuator part consists of an effective mass m_p , a viscous linear damper c_p , and a linear spring k_p . The displacement of piezoelectric actuator is δ . The flexure, extension bar, tool holder and cutting tool are represented by a lumped mass m_f , a linear spring k_f and a viscous linear damper c_f . The coordinate x_p describes the relative displacement of the tool part with respect to the electrohydraulic actuator and x_h represents the position of electrohydraulic actuator. The piston of the electrohydraulic actuator has mass m_h and is moved by the force F_h generated by the pressure difference. P is the preload which makes the piezoelectric actuator remain in compression and F_{cut} represents cutting force.

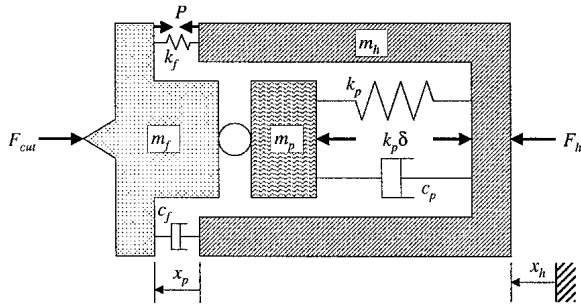


Figure 2: Model of the Dual Stage Actuator

A mathematical MIMO model of the dual stage actuator system in Figure 2 can be found in [5]. The dynamic equations contain many electrohydraulic servovalve design parameters from [2]. Even though a mathematical MIMO model is available, there is not enough information about the electrohydraulic actuator design parameters which we need to build a model. Thus, in this paper we use frequency response tests and least squares fit to obtain a model. The frequency responses are shown in Figure 3, 4, 5, and 6. As we can see, the dynamic effects of the piezoelectric actuator voltage input to the electrohydraulic actuator output are negligible.

Let's examine whether the system stability can be obtained through two SISO controllers for each actuator. Let G_p , G_h and G_{ph} represent actuator transfer functions of piezoelectric, electrohydraulic, electrohydraulic to piezoelectric, respectively. If u_p is the control signal to the piezoelectric actuator and u_h is to the hydraulic actuator, then the displacements x_p and x_h are

$$\begin{bmatrix} x_p \\ x_h \end{bmatrix} = \begin{bmatrix} G_p & G_{ph} \\ 0 & G_h \end{bmatrix} \begin{bmatrix} u_p \\ u_h \end{bmatrix} = \mathbf{G} \begin{bmatrix} u_p \\ u_h \end{bmatrix}. \quad (1)$$

In the structure of cascaded two SISO controllers, the controller for the electrohydraulic actuator calculates the control effort u_h with the electrohydraulic actuator error $e_h = r - x_h$, where r is reference. If e_h is fed to the piezoelectric actuator as reference and the control signal u_p is computed from the piezoelectric actuator error $e_p = e_h - x_p$,

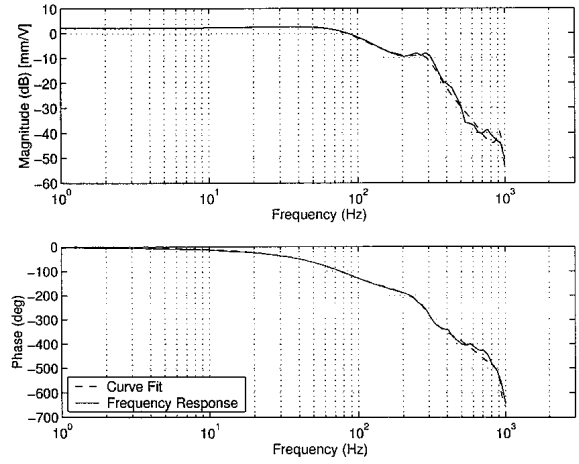


Figure 3: Frequency Response of the Electrohydraulic Actuator

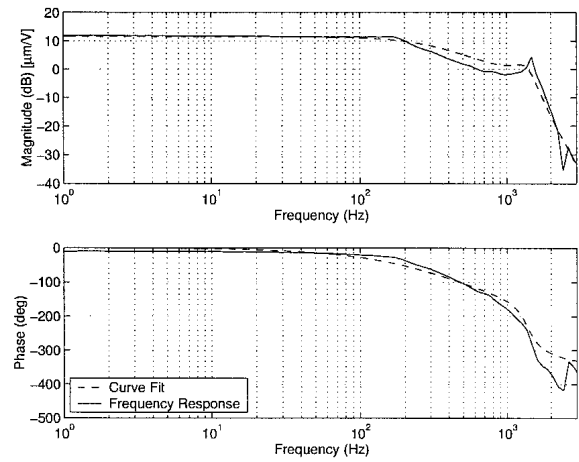


Figure 4: Frequency Response of the Piezoelectric Actuator

then

$$u_h = K_h (r - x_h), \quad u_p = K_p (r - x_h - x_p),$$

$$\begin{bmatrix} u_p \\ u_h \end{bmatrix} = - \begin{bmatrix} K_p & K_p \\ 0 & K_h \end{bmatrix} \begin{bmatrix} x_p \\ x_h \end{bmatrix} + \Delta = -\mathbf{K} \begin{bmatrix} x_p \\ x_h \end{bmatrix} + \Delta, \quad (2)$$

where K_h , K_p are controllers for each actuator and Δ contains reference-related terms. The characteristic equation of the closed-loop system is

$$\begin{aligned} \det(\mathbf{I} + \mathbf{K}\mathbf{G}) &= \det \left(\mathbf{I} + \begin{bmatrix} K_p G_p & K_p (G_h + G_{ph}) \\ 0 & K_h G_h \end{bmatrix} \right) \\ &= \det(1 + K_p G_p) \cdot \det(1 + K_h G_h) \\ &= 0 \end{aligned} \quad (3)$$

Eq. (3) shows that the closed-loop poles are determined by two SISO control loops. Thus, the system stability can be guaranteed without knowing G_{ph} .

The electrohydraulic actuator is modeled as a 8th order system and the piezoelectric actuator as a 5th order system. The frequency components of references for the noncircular

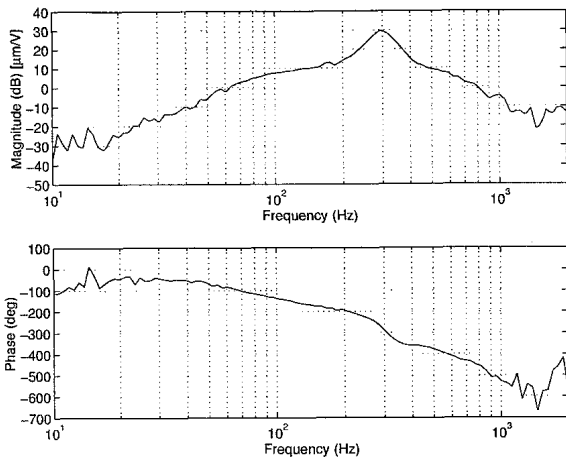


Figure 5: Frequency Response - Electrohydraulic Actuator Voltage Input to Piezoelectric Actuator Feedback Output

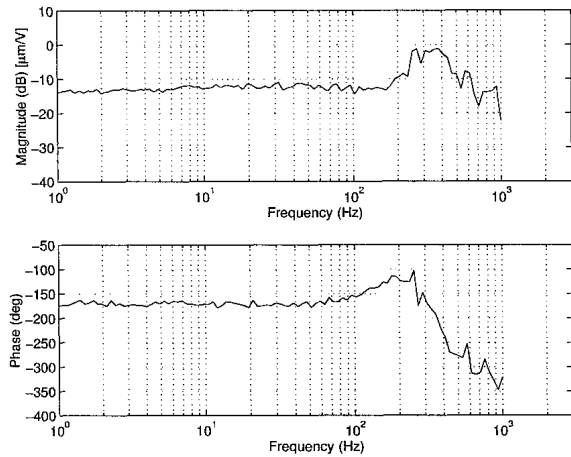


Figure 6: Frequency Response - Piezoelectric Actuator Voltage Input to Electrohydraulic Actuator Feedback Output

cam turning are mainly in the low frequency range. Thus, the influence of the electrohydraulic actuator dynamics on the piezoelectric actuator, which is described in Figure 5 in relatively high frequency range, is neglected in this paper to ease the control system design and to reduce the implementation complexity. Two independent SISO systems are considered in robust repetitive controller design.

3 Robust Repetitive Controller Design

The controller for the dual stage actuator system is constructed by two parameter robust repetitive control (TPRRC) [4] design method. In this method, the high order delay term in the periodic signal generator is treated as a fictitious uncertainty and discrete-time μ -synthesis is applied.

TPRRC design structure is shown in Figure 7, where $G(z)$ is a plant, $q(z, z^{-1})$ is a zero phase lowpass filter, and $W_r(z)$ and $W_p(z)$ are input multiplicative uncertainty weighting

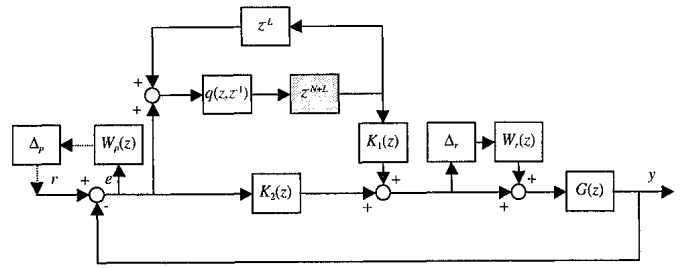


Figure 7: μ -Synthesis Block Diagram of TPRRC Method

function and performance weighting function, respectively. N is the period of the periodic signal. In the traditional zero phase error tracking control (ZPETC) type repetitive controller design method [7], L is the sum of the plant delay and the controller delay which comes from inversion of unstable zero part in plant, but in TPRRC, L is not well defined. Roughly speaking, L is assigned with a value of around 10 and it produces satisfying results in most of cam turning applications. $K_1(z)$ and $K_2(z)$ are controller blocks to be designed via discrete-time μ -synthesis technique. Discrete-time μ -synthesis is performed with the big delay term z^{-N+L} replaced by a fictitious uncertainty Δ_f . Otherwise, z^{-N+L} term leads to very high order controllers, $K_1(z)$ and $K_2(z)$. For example, if we use a 6kHz sampling rate at spindle speed of 600rpm, then $N = 600$. That means the order of the controller designed by μ -synthesis will be well beyond of 600. It may not work in practice. The final augmented block structure of uncertain perturbations including the fictitious uncertainty, $\hat{\Delta}$ is

$$\hat{\Delta} = \begin{bmatrix} \Delta_f & 0 & 0 \\ 0 & \Delta_r & 0 \\ 0 & 0 & \Delta_p \end{bmatrix}. \quad (4)$$

Assume nominal stability such that $M = F_l(P, [K_1, K_2])$ is (internally) stable, robust performance is obtained if $\mu_{\hat{\Delta}}(M) < 1$. See [8] for details.

It is important to check μ_{Δ_r} value for robust stability with z^{-N+L} , $K_1(z)$ and $K_2(z)$ after getting controllers from μ -synthesis, because $\mu_{\hat{\Delta}}$ contains some amount of conservatism due to the fictitious uncertainty block. Some controllers having $\mu_{\hat{\Delta}}$ values of greater than one in D - K iteration may show $\mu_{\Delta_r} < 1$ and be safe in use. Since nominal performance of repetitive controllers is evaluated at the fundamental frequencies, robust performance test including Δ_p is not crucial, but $W_p(z)$ can be used to enforce non-periodic disturbance rejection in the low frequency range.

Figure 8 shows the controller block diagram for the dual stage actuator system, where $G_p(z)$ and $G_h(z)$ are the piezoelectric actuator and the electrohydraulic actuator, respectively. The corresponding controller blocks, TPRRC_p and TPRRC_h are built separately and cascaded together under the assumption that there is little interaction between two actuator systems. The following equation shows that the total error is the same as e_p if the electrohydraulic actuator error e_h is small enough to fit in the travel length of piezo-

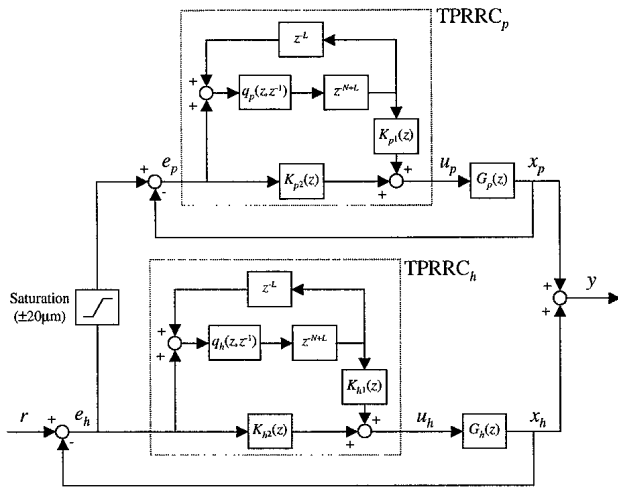


Figure 8: Block Diagram of the Control System

electric actuator ($\pm 20\mu\text{m}$) so that there is no reference saturation.

$$\begin{aligned} e &= r - y \\ &= r - (x_h + x_p) \\ &= e_h - x_p \\ &= e_p \end{aligned}$$

The design results in terms of sensitivity functions and design parameters for each actuator are shown in Figure 9 and Figure 10 when sampling rate is 6kHz and spindle speed is 600rpm ($N = 600$, $L = 10$).

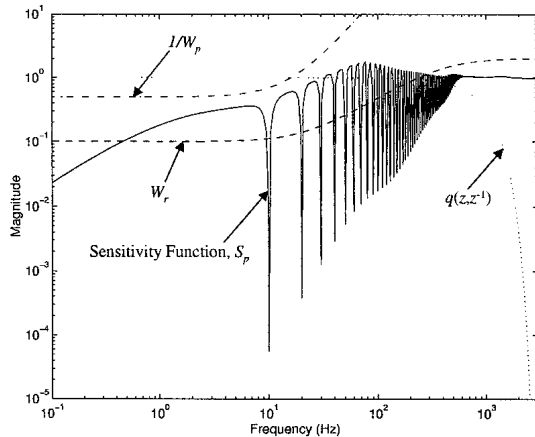


Figure 9: Design for the Piezoelectric Actuator

The sensitivity function describes the relation from (periodic) reference to tracking error. The error e_h in the electrohydraulic actuator is used as reference for the piezoelectric actuator system. Therefore, the cascaded configuration in Figure 8 produces the following relation.

$$e_p = S_p e_h = S_p S_h r \quad (5)$$

Since the final tracking error is the same as e_p , the overall sensitivity function is the product of two sensitivity functions. The overall sensitivity function has much deeper

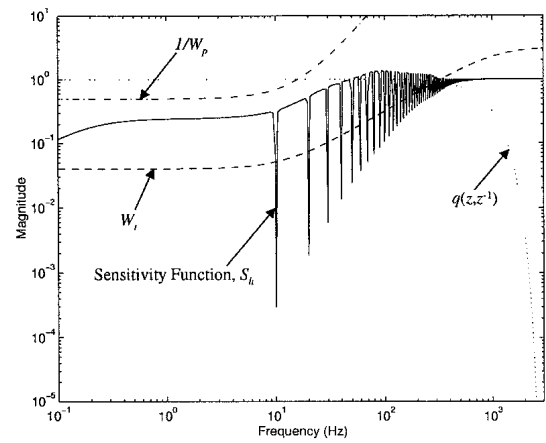


Figure 10: Design for the Electrohydraulic Actuator

notches at the fundamental frequencies through multiplication of two sensitivity functions and furthermore, it reveals disturbance rejection in the low frequency range against non-periodic disturbances, which comes from two $1/W_p(z)$ weights pushing down S_p and S_h in each TPRRC design procedure.

4 Simulation and Experimental Results

In this section, we present simulation and experimental results from the dual stage actuator system for the noncircular cam turning process. The controllers were implemented on a 32 bits floating point TMS320C32 DSP board and the position feedback signal from the electrohydraulic actuator was collected by a laser encoder with a $0.6\mu\text{m}$ resolution. The relative displacement of the piezoelectric actuator was measured using an inductive position probe whose resolution was $0.1\mu\text{m}$, but the noise level of the probe after a lowpass filter was $0.5\mu\text{m}$. A sampling rate 6kHz was adopted. The designed controllers initially had the 46th and 45th order for the piezoelectric actuator and the electrohydraulic actuator, respectively. Reduced 9th order controllers were implemented for both actuator systems in experiments. Even though a lowpass $q(z, z^{-1}) = [0.25z + 0.5 + 0.25z^{-1}]^4$ was used during μ -synthesis for both actuator systems to achieve appropriate level of $\mu_{\Delta}(M)$ values, more aggressive $q(z, z^{-1})$ filters could be employed in experiments until each actuator servo control system showed instability. The zero phase lowpass $q_p(z, z^{-1}) = [0.1z + 0.8 + 0.1z^{-1}]$ and $q_h(z, z^{-1}) = [0.25z + 0.5 + 0.25z^{-1}]$ filters were used for the piezoelectric actuator and the electrohydraulic actuator, respectively. Two cam profile references are represented in Figure 11. The mild cam profile was used with a spindle speed of 600rpm ($N = 600$) and for the sharp cam profile, a 300rpm spindle speed was tested ($N = 1200$). Note that in TPRRC design procedure, Z^{-N+L} is replaced by a fictitious uncertainty, so the different N values don't require a new controller design. Figure 12 shows normalized power spectrums of two cam profiles shown in Figure 11. The cam pro-

files are periodic with the period of 10Hz and 5Hz respectively, therefore their spectrums appear at their fundamental frequencies by the sampling theorem. In either cam profile, the frequency components in the high frequency range are not dominant.

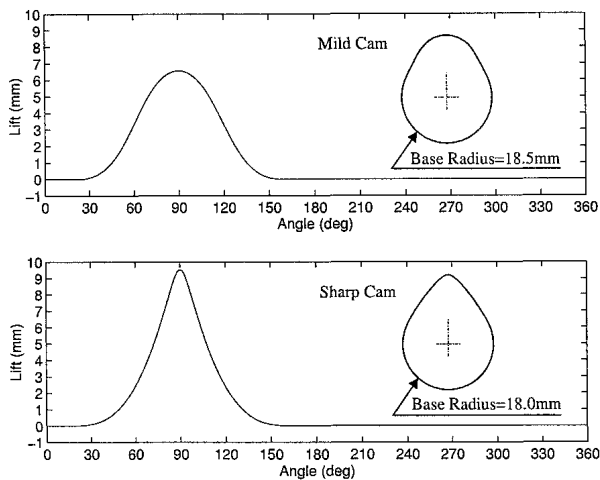


Figure 11: Two Cam Profiles

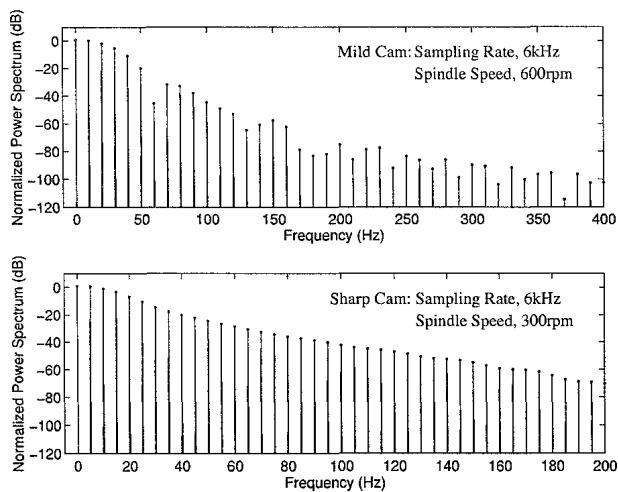


Figure 12: Normalized Power Spectrums of Two Cam Profiles

Figure 13 represents simulation results when the cam profile reference is perfectly split and used separately. The mild cam profile shown in Figure 11 is split at a frequency of 100Hz. The low frequency part (Fig. 13(b)) and the high frequency part (Fig. 13(c)) construct the original mild cam profile (Fig. 13(a)). Since the rectangular window function is used to split the frequency spectrum at 100Hz, we can see oscillatory behavior in time domain signals (Fig. 13(b) and (c)). Let's assume that the piezoelectric actuator perfectly follows its reference generated only with the high frequency part, which magnitude is within $\pm 20\mu\text{m}$ and it is appropriate for the piezoelectric actuator travel length. The tracking performance of the electrohydraulic actuator servo system is tested in simulation with two references, the one is the original mild cam profile (Fig. 13(a)) and the other

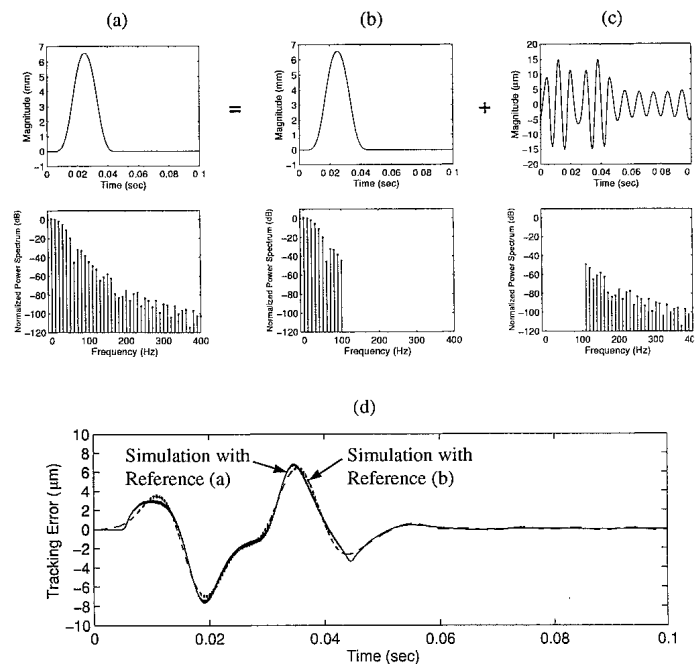


Figure 13: Simulation Results: Tracking Performance of the Electrohydraulic Actuator with (Low) Frequency-Limited Reference (Mild Cam, 6kHz, 600rpm)

is the low frequency-limited cam profile (Fig. 13(b)). The results are compared in Figure 13(d). We can see that the tracking performance improvement is not significant in the electrohydraulic actuator servo system even when it deals with only the low frequency-limited reference. It implies that the tracking performance in the noncircular cam turning process lies in how to make the notches deeper at low fundamental frequencies in the control system's sensitivity function curve rather than how to enlarge its bandwidth to higher frequencies. It also justifies our approach which is cascading two actuator servo systems to have the squaring effect on the overall sensitivity function.

Figure 14 and 15 show the steady-state tracking performance for the mild cam profile at 600rpm and the sharp cam profile at 300rpm, respectively. Because the error from the electrohydraulic actuator is not pure periodic and it may be too big for the reference of the piezoelectric actuator while converging to its steady-state, the moving average of 5 consecutive cycles of e_h was used as the reference for the second stage and the reference magnitude was truncated with the limits of $\pm 20\mu\text{m}$. The total errors in Figure 14 and Figure 15 were calculated accordingly. Previous research [6] with a single stage electrohydraulic system and a 5.12kHz sampling rate, reported maximum tracking errors around $7\mu\text{m}$ for the mild cam profile at 600rpm and around $25\mu\text{m}$ for the sharp cam profile at 300rpm. We can see the tracking performance improvement through the dual stage actuator system.

The transient behavior of the dual stage actuator system is shown in Figure 16 in terms of RMS (root-mean-square) error values. This experiment was carried out with the mild

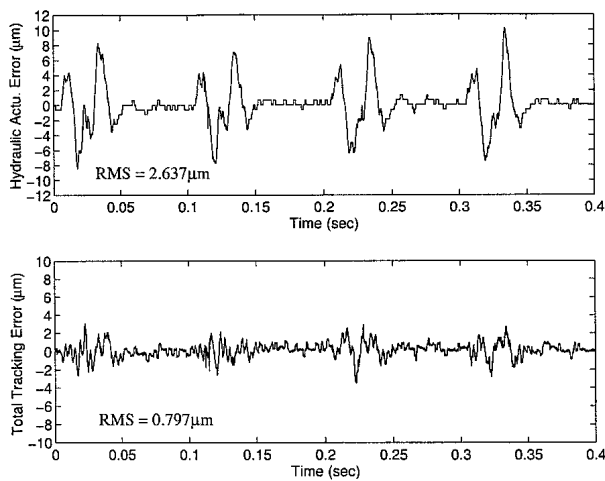


Figure 14: Experimental Results with Mild Cam Profile

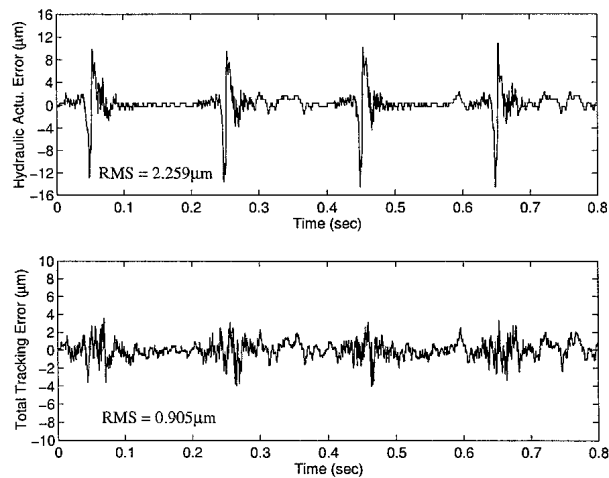


Figure 15: Experimental Results with Sharp Cam Profile

cam profile at spindle speed of 600rpm. The RMS error values were calculated at every cycle from the time when both actuators in the dual stage actuator system were turned on simultaneously. The RMS value of total tracking error reduced to less than $5\mu\text{m}$ at around 50 cycles (equivalently within 5 seconds) and converged to its steady-state value of approximately $0.8\mu\text{m}$ within 100 cycles (equivalently within 10 seconds).

5 Conclusions

A discrete-time robust repetitive controller was designed for a dual stage actuator system for the noncircular cam turning process. Cascading the two SISO repetitive controllers designed separately for two actuator systems produces a squaring effect on the overall sensitivity function. Simulation shows the effects of frequency-limited reference are minimal and it justifies the cascading two servo systems approach. Experimental results of the dual stage actuator system demonstrated the tracking performance improvement in

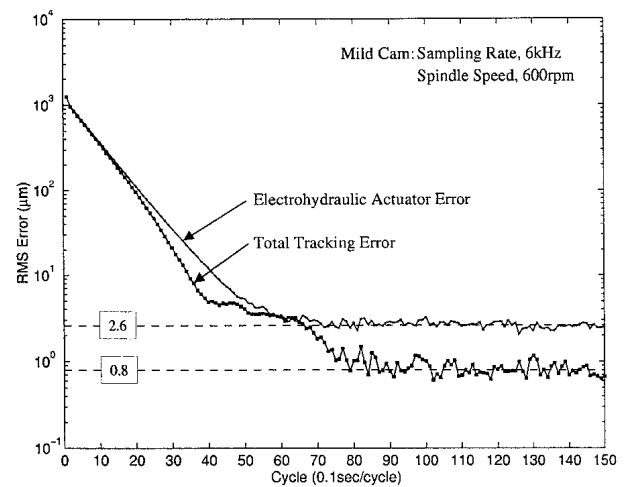


Figure 16: Experimental Results: Transient RMS Errors

the noncircular cam turning process.

References

- [1] Aggarwal, S. K., Horsley, D. A., Horowitz, R., and Pisano, A. P., "Micro-actuators for High Density Disk Drives", *Proceedings of American Control Conference*, Albuquerque, New Mexico, pp. 3979-3984, 1997.
- [2] Kim, D. H., and Tsao, T.-C., "A Linearized Electrohydraulic Servo Valve Model for Valve Dynamics Sensitivity Analysis and Control System Design", *ASME Journal of Dynamic Systems, Measurement, and Control*, Vol. 122, pp. 179-187, March 2000.
- [3] Koganezawa, S., Uematsu, Y., and Yamada, T., "Dual Stage Actuator System for Magnetic Disk Drives Using a Shear Mode Piezoelectric Microactuator", *IEEE Transactions on Magnetics*, Vol. 35, pp. 988-992, March 1999.
- [4] Li, J., and Tsao, T. C., "A Two Parameter Robust Repetitive Control Design Using Structured Singular Values", *Proceedings of the 37th IEEE Conference on Decision and Control*, Tampa, Florida, pp.1230-1235, December 1998.
- [5] Li, J., "Robust Repetitive Control and Its Application", Ph.D. Dissertation, University of Illinois at Urbana-Champaign, Department of Mechanical and Industrial Engineering, 1999.
- [6] Tsao, T. C., Hanson, R. D., Sun, Z., and Babiniski, A., "Motion Control of Non-Circular Turning Process for Camshaft Machining", *1998 Japan-USA Symposium on Flexible Automation*, Otsu, Japan, pp. 485-489, July 1998.
- [7] Tomizuka, M., Tsao, T. C., and Chew, K. K., "Analysis and Synthesis of Discrete-Time Repetitive Controllers", *ASME Journal of Dynamic Systems, Measurement, and Control*, Vol. 111, pp. 353-358, September 1989.
- [8] Zhou, K., Doyle, J. C., and Glover, K., *Robust and Optimal Control*, Prentice-Hall, Upper Saddle River, 1996